

PolyCOFs: A New Class of Freestanding Responsive Covalent Organic Framework Membranes with High Mechanical Performance

Zhifang Wang,[†] Qi Yu,[†] Yubo Huang,[‡] Hongde An,^{§,||} Yu Zhao,[†] Yifan Feng,^{§,||} Xia Li,[†] Xinlei Shi,[#] Jiajie Liang,[#] Fusheng Pan,[∇] Peng Cheng,^{†,||} Yao Chen,^{*,§,||} Shengqian Ma,^{*,‡} and Zhenjie Zhang^{*,†,§}

[†]College of Chemistry, Nankai University, Tianjin 300071, People's Republic of China

[‡]Department of Chemistry, University of South Florida, 4202 East Fowler Avenue, Tampa, Florida 33620, United States

[§]State Key Laboratory of Medicinal Chemical Biology, Nankai University, Tianjin 300071, People's Republic of China

^{||}College of Pharmacy, Nankai University, Tianjin 300071, People's Republic of China

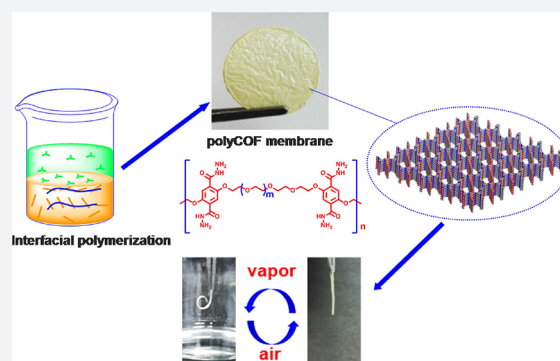
[‡]College of Precision Instrument and Optoelectronics Engineering, Tianjin University, Tianjin 300072, People's Republic of China

[#]School of Materials Science and Engineering, Nankai University, Tianjin 300071, People's Republic of China

[∇]School of Chemical Engineering and Technology, Tianjin University, Tianjin 300072, People's Republic of China

Supporting Information

ABSTRACT: Traditional covalent organic frameworks (COFs) are prepared via polymerization based on small molecular monomers. However, the employment of polymers as building blocks to construct COFs has not been reported yet. Herein, we create a new concept of polymer covalent organic frameworks (polyCOFs) formed by linear polymers as structural building blocks, which inherit the merits from both COFs and linear polymers. PolyCOFs represent a new category of porous COF materials that demonstrate good crystallinity and high stability. More importantly, benefiting from the flexibility and processability of a linear polymer, polyCOFs can spontaneously form defect-free, flexible, and freestanding membranes that exhibit excellent mechanical properties and undergo reversible mechanical transformation upon exposure to various organic vapors. For the first time, we demonstrated that polyCOF membranes can be used as artificial muscles to perform various complicated motions (e.g., lifting objects, doing “sit-ups”) triggered by vapors. This study bridges the gap between one-dimensional amorphous linear polymers and crystalline polymer frameworks and paves a new avenue to prepare stimuli-responsive actuators using porous COF materials.



INTRODUCTION

Covalent organic frameworks (COFs) represent an emerging class of well-defined crystalline materials with ordered structures, good chemical stability, high porosity, and tunable pore size.^{1–7} Featuring these advantages, COFs have demonstrated great potentials for applications in many fields such as catalysis,^{8,9} membrane separation,¹⁰ gas storage,¹¹ drug delivery,¹² supercapacitors,¹³ and functional devices.¹⁴ Since the first COF reported in 2005,¹⁵ a variety of COFs have been prepared using appropriate organic building blocks (e.g., monomers with boric acid, aldehyde, amino groups) and covalent linkages such as boronate,¹⁵ imine,¹⁶ hydrazone,¹⁷ and sp² carbon.^{18,19} However, there remain some issues and limitations that hinder the practical applications of COFs such as fabricating them for large electronic devices²⁰ and preparing them as macroscale membranes for gas separation, water treatment, or fuel cells.²¹ (i) COFs typically exist as nano- or micron-sized crystalline powders due to their internal

structural defect which prevents them from forming large crystals or continuous membranes. (ii) Traditional COFs possess poor processability resulting from their infusibility in common solvents and brittleness. To overcome this issue, methods including interfacial polymerization of small monomers,^{22–24} vacuum filtration,²⁵ and utilization of *p*-toluene-sulfonic acid as a molecular organizer^{26,27} have been employed to prepare freestanding COF membranes. However, most COF membranes showed weak mechanical properties and processability which restrict their further applications. Therefore, exploring new strategies to prepare freestanding membranes with good processability and mechanical properties is of great significance and will vastly broaden the applications of COFs and open up new avenues to overcome present limitations.

Received: March 3, 2019

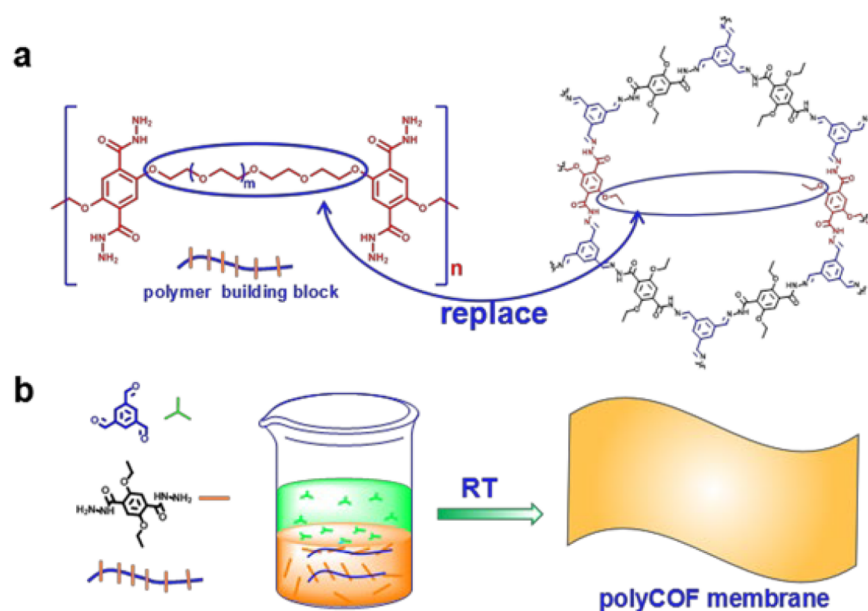


Figure 1. (a) Strategy to fabricate the polyCOF analogue of COF-42 via replacing dangling $-OCH_2CH_3$ groups by PEG linkers. (b) Illustration of a new concept to fabricate the freestanding polyCOF membrane via a three-component condensation.

Amorphous, linear polymers [e.g., PIM-1, poly(ether imide), poly(vinyl alcohol)] have been widely used to fabricate polymer/porous-material hybrid membranes for separation, drug delivery, and smart devices because of their good mechanical properties and excellent processability.^{28–30} Distinct from the conventional mixed matrix membrane (MMM) approach which suffers from weak filler–polymer interaction and unavoidable defects,^{31–33} directly using linear polymers as building blocks for porous materials can overcome the drawbacks of MMMs and afford a new class of hybrid materials harnessing not only the advantages of linear polymers such as facile membrane formation, good processability, and high chemical stability but also the excellent properties of porous materials, such as structural robustness, well-defined structures, and permanent porosity. For example, Cohen and co-workers have demonstrated that directly using linear polymers as ligands to coordinate with metal ions can afford polymer–metal–organic-framework (polyMOF) hybrid materials.³⁴ However, polyMOF materials typically exist as nanosized crystalline powders. Fabricating macroscale, freestanding, flexible membranes using the polyMOF approach has not been successfully achieved yet. Inspired by the structural versatility of COFs and advantages of linear polymers, we postulate the possibility to use linear polymers as building blocks to directly construct COF membranes—referred to as a new concept of polyCOF membranes. Distinct from the traditional pure COF membranes, the introduced linear polymers will endow polyCOF membranes new properties, such as enhanced mechanical performance and stimuli response. To realize the concept of polyCOF, we chose highly porous and stable hydrazone-based COFs, COF-42, as an eminent representative. COF-42 was first reported by Yaghi in 2011¹⁷ prepared via a hydrothermal condensation reaction of 1,3,5-triformylbenzene (TB) and 2,5-diethoxyterephthalohydrazide (DTH). A close examination of COF-42 indicates that the flexible $-OCH_2CH_3$ chains dangling from DTH linker point into the channel center. Therefore, a potential approach to make polyCOF analogues of COF-42 would be to tether

terephthalohydrazide moieties together across the pore space with polymer chains to form polyCOFs (Figure 1a).

In this study, PEGylated linear polymers were first used as structural building blocks to fabricate COFs, which can facilitate the formation of defect-free, macroscale, and freestanding polyCOF membranes under ambient conditions. Tuning the content of polymer building blocks, the crystallinity, porosity, thickness, and mechanical properties of polyCOF membranes can be readily adjusted. Interestingly, polyCOF membranes exhibited reversible bending behaviors responsive to various organic vapors, making them behave as artificial muscles with various muscle motions, including lifting objects and doing “sit-ups” triggered by vapor stimuli. This study points out a new concept to fabricate a new class of advanced COF materials that combined the merits of both COFs and linear polymers, thereby further broadening the applications of COFs.

RESULTS AND DISCUSSION

Design and Synthesis of PolyCOFs. To prepare polyCOF analogues of COF-42, a water-soluble, linear polymer (DTH-POLYMER) containing DTH moieties in the backbone was designed and prepared using step-growth polymerization and purified via a dialysis method (molecular weight cutoff, 2000 g/mol). PEG400 ($M_w = 400$ g/mol) was adopted as the polymer linkage which possesses a chain length longer than the farthest distance among dangling $-OCH_2CH_3$ groups (Figure S1). Furthermore, polymer building blocks containing polyethylene glycols can improve its water solubility thus facilitating the formation of membranes via interfacial polymerization. Both 1H and ^{13}C NMR verified the composition of the polymers. The molecular weight values of as-synthesized polymers were determined by gel permeation chromatography (GPC) (Figure S2). The results revealed that the DTH-400 in ester form possessed M_n values of 8343 g/mol, M_w values of 12 578 g/mol, and polydispersity index (PDI) of 1.51.

As illustrated in Figure 1b, a multicomponent condensation reaction was employed to prepare polyCOFs (poly_xCOF-42 series) with hydrazone linkages via an interfacial polymerization of DTH-400 and DTH of different molar ratios ($x = [\text{DTH-400}]/([\text{DTH}] + [\text{DTH-400}])$) with TB at room temperature. The hydrazine moieties (DTH+DTH-400) were first dissolved in mixed solvent of water and dioxane as a bottom layer; meanwhile, TB was dissolved in mesitylene as an upper layer. A liquid–liquid interface was then formed between immiscible water and mesitylene. In this interfacial reaction, dioxane solvent played an important role: (i) Dioxane serves as a special solvent that can promote the dissolution of hydrazine. (ii) Dioxane is miscible with both water and mesitylene, which allows efficient mass transfer between bottom and upper layers. In addition, acetic acid was added to the mesitylene layer as a catalyst to control the reaction rate and improve the crystallinity of COFs. The polymerization reaction of aldehyde and hydrazine was then performed on the solvent interface to afford COF membranes (Figure S3) under ambient conditions for ~48 h. Notably, all reactions possessed >80% yields, which are comparable to the reported yield of COF-42 (78%) under solvothermal conditions^{17,35} and higher than those of reported COF membranes fabricated via the interfacial polymerization method.^{22–24}

Characterization of PolyCOF Membranes. A series of polyCOF membranes were obtained via varying the polymer contents of DTH-400. Freestanding membranes can be harvested and easily transferred onto arbitrary substrates (e.g., filter paper, glass, silicon plate) (Figure 2 and Figure

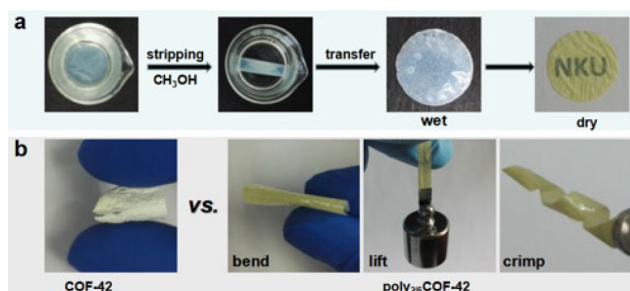


Figure 2. (a) Illustration of the process to harvest polyCOF membranes. (b) Comparison of the mechanical properties of COF-42 vs poly_{2/6}COF-42.

S3). The pristine COF-42 (without adding DTH-400) obtained via the same interfacial polymerization method formed an opaque and brittle membrane which was apt to break or crack during bending process (Figure 2 and Movie S1), indicative of a weak mechanical property. With the increase of the contents of DTH-400 ($x = 1/6–1$) (Figure S3), the formed poly_xCOF-42 membranes became more optically transparent, and the flexibilities of poly_xCOF-42 membranes were significantly enhanced. For instance, poly_{2/6}COF-42 membranes can be repeatedly bent, twisted or stretched without damage (Figure 2b and Movie S2). Moreover, after these mechanical treatments, the polyCOFs still retain their crystallinity and porosity (Figure S4).

The crystallinity of membranes was determined by powder X-ray diffraction (PXRD) measurements. PXRD patterns of poly_xCOF-42 ($x = 1/6–5/6$) possessed the characteristic peaks ($2\theta = 3.4^\circ$, 7.0° , and 26.9°) of pristine COF-42.¹⁷ As shown in Figure 3a, among the different contents of DTH-400,

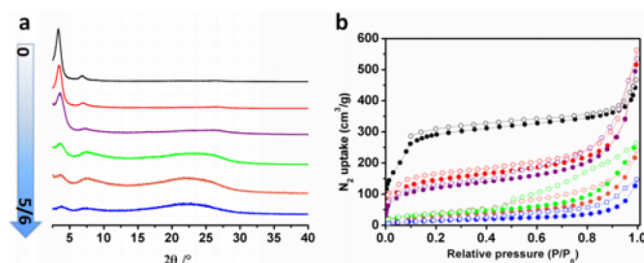


Figure 3. (a) PXRD patterns. (b) N₂ sorption isotherms: black (COF-42), red (poly_{1/6}COF-42), purple (poly_{2/6}COF-42), green (poly_{3/6}COF-42), orange (poly_{4/6}COF-42), and blue (poly_{5/6}COF-42).

poly_{1/6}COF-42 and poly_{2/6}COF-42 exhibited the best crystallinity comparable to pristine COF-42. It could be presumably due to the fact that PEG chains can be orderly located in COF's hexagonal channels without forming PEG chain entanglement. However, with an increase in the contents of DTH-400 ($x = 3/6–5/6$) in poly_xCOF-42, PEG chains would form interlayer or intralayer chain entanglement (Figure S5), which will unavoidably block COF's channels and partially undermine the crystallinity of COF's frameworks. Moreover, the introduced PEG chains would disturb the π – π stacking interactions among the layers in the extended polyCOF, which would lead to decrease of PXRD peak intensity and peak broadening.³⁶ As predicted, the intensity of the characteristic PXRD peaks of poly_xCOF-42 ($x = 3/6–5/6$) gradually decreased, and meanwhile, the intensity of a broad amorphous peak at $2\theta \approx 22^\circ$ gradually increased. In addition, it is found that polyPEG-400 with full loading of polymer building units was completely amorphous with a broad peak centered at $2\theta \approx 22^\circ$ (Figure S6).

FT-IR spectra of the poly_xCOF-42 (Figures S7 and S8) showed the stretching modes at 1620–1610 and 1225–1215 cm⁻¹ associated with the formation of the —C=N— bonds, which agrees well with the corresponding values of COF-42. It is notable that the disappearance of the carbonyl stretching modes (1688 cm⁻¹) of the aldehyde groups clearly suggested the complete reaction of starting materials. The atomic-level construction of poly_xCOF-42 was further confirmed by solid-state ¹³C NMR spectroscopy (Figure S9). The characteristic peak at 150 ppm in all test materials can be attributed to the formation of —C=N— bonds. We observed that, with increasing contents (x) of DTH-400, the peaks of ethyl groups from DTH at 13 and 65 ppm gradually disappeared, and a new peak (71 ppm) ascribed to the carbons in PEG groups appeared, indicating the existence of polymer building blocks in poly_xCOF-42. In addition, PXRD patterns revealed that the representative material, poly_{2/6}COF-42, can retain its crystallinity and structural integrity (Figure S10) after treatment with 1 M NaOH, 6 M HCl, boiling water, or various organic solvents (e.g., DMF, MeOH) for 5 days, indicative of its high chemical stability and potential nanofiltration applications in various solvent systems.

SEM images (Figure 4a) revealed that COF-42 membranes possessed rough surfaces with significant defects and voids packed by nanorod particles, which were further confirmed by the transmission electron microscopy (TEM) (Figure S12). Notably, poly_xCOF-42 membranes possessed uniform, smooth, and defect-free surfaces with compact and cohesive structures (Figure 4b and Figure S11). TEM images revealed that the dispersed poly_xCOF-42 after sonication treatment

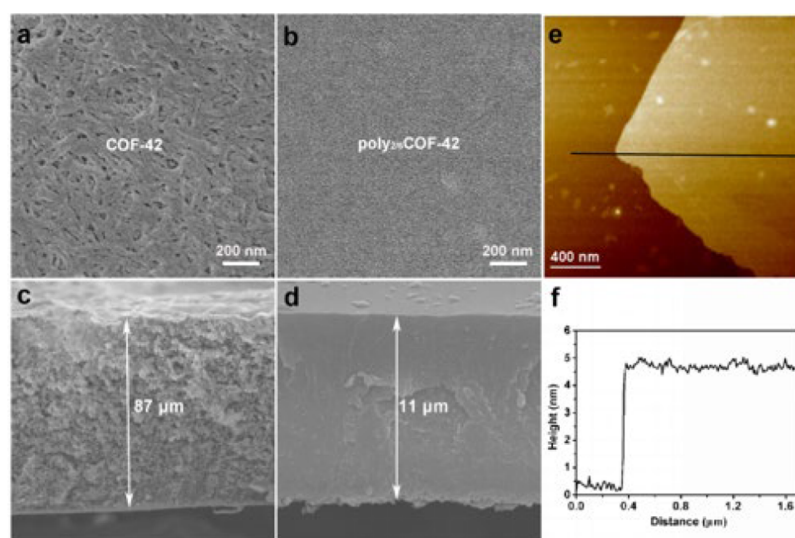


Figure 4. Top view SEM images of the freestanding membranes with (a) COF-42 and (b) $\text{poly}_{2/6}\text{COF-42}$. Cross-section SEM images of (c) COF-42 and (d) $\text{poly}_{2/6}\text{COF-42}$. (e) AFM image of the $\text{poly}_{2/6}\text{COF-42}$ thin film and (f) corresponding height profile showing a thickness of 4.5 nm using a low precursor concentration.

displayed sheetlike particles (Figure S12). In addition, SEM images of the cross-section of membranes (Figure 4c,d and Figure S11) further proved the compact and cohesive particle packing nature of $\text{poly}_x\text{COF-42}$ membranes and a relative loose particle packing in COF-42. These results indicate that the linear polymers in the COF structure may serve as threads to interlace and bond COF particles, which facilitate the formation of highly flexible and defect-free membranes. Furthermore, we found that the thickness of the polyCOF membranes can be easily tuned via varying the initial concentration of reactants (for more details, see the Supporting Information). For example, we have successfully fabricated a film as thin as 4.5 ± 0.3 nm using a low precursor concentration (Figure 4e,f, Figure S13).

N_2 sorption isotherms at 77 K were examined to evaluate the porosity and pore size of polyCOFs. The parent COF-42 membrane possessed surface areas of $951 \text{ m}^2/\text{g}$ (BET), comparable to the reported value of COF-42 prepared by solvothermal synthesis. The surface areas of $\text{poly}_x\text{COF-42}$ gradually decreased from 479 to $56 \text{ m}^2/\text{g}$ (Figure 3b) with the increase of the polymer content (x) from 1/6 to 5/6. The pore size distribution was calculated by density functional theory (DFT) methods (Figure S14), and COF-42 possesses a narrow pore size distribution of $\sim 24 \text{ \AA}$, in good agreement with the reported value of 23 \AA and structure simulation. Ascribed to the cross-linking effect of linear polymers in $\text{poly}_x\text{COF-42}$, the pores of $\sim 24 \text{ \AA}$ from COF-42 disappeared, and new pores centered at $\sim 13 \text{ \AA}$ appeared. The tailored narrow pores are expected to benefit the nanofiltration performance of polyCOF membranes.^{21–23} We found that, after tailoring the pore apertures, all polyCOF membranes exhibited high water permeance and much better separation efficiency than pristine COF-42 membranes (Tables S1–S3). Selecting $\text{poly}_{2/6}\text{COF-42}$ membrane as a representative, we conducted filtration experiments using water contaminated with dyes. Coomassie brilliant blue R-250 aqueous solution ($10 \mu\text{M}$) can be quickly separated by the $\text{poly}_{2/6}\text{COF-42}$ membrane under 1 bar pressure. Dye concentrations in the feed and permeate were analyzed by UV–vis spectrometer revealing >99% removal of the Coomassie brilliant blue R-250,

which showed much better separation performance than the pure COF-42 membrane (65%) (Figures S15–S17). Furthermore, the $\text{poly}_{2/6}\text{COF-42}$ membrane was subjected to a mixed feed of Coomassie brilliant blue R-250 ($M_w = 854 \text{ g/mol}$; $\sim 1.8 \text{ nm} \times 2.3 \text{ nm}$) and methyl orange ($M_w = 327 \text{ g/mol}$; $\sim 1.1 \text{ nm} \times 0.4 \text{ nm}$). It only allowed the passage of the methyl orange (yellow). The eluent was further analyzed by UV–vis spectroscopy which showed that the Coomassie brilliant blue R-250 was completely rejected, and the methyl orange of >99% purity was recovered (>96%) from the filtrate (Figure S18). By contrast, the COF-42 membrane cannot completely separate the two dyes (Figure S19). Moreover, the $\text{poly}_{2/6}\text{COF-42}$ membrane showed good reusability (Figures S20–S23).

Exploration of the Generality of the PolyCOF Membranes Approach. To explore the generality of the polyCOF approach to fabricate freestanding COF membranes, we designed and synthesized DTH-600 (Figure S24) to replace DTH-400 under identical conditions, and obtained a series of $\text{poly}_x\text{COF-42}^*$ membranes (Figure S25). For example, we obtained a defect-free and freestanding membrane of $\text{poly}_{2/6}\text{COF-42}^*$ with a highly crystalline nature: the PXRD pattern matched well with the parent COF-42 (Figure S26). Notably, the polyPEG-600 membrane with full loading of DTH-600 showed moderate crystallinity that further proved the possibility to completely use linear polymers as building units to directly construct crystalline COFs. Solid-phase ^{13}C NMR (Figure S27) and FT-IR spectra (Figures S28 and S29) further confirmed the existence of hydrazone linkages in $\text{poly}_{2/6}\text{COF-42}^*$. N_2 sorption isotherms revealed that $\text{poly}_{2/6}\text{COF-42}^*$ possessed a Langmuir surface area of $350 \text{ m}^2/\text{g}$, which was lower than that of PEG400 (Figure S30). It could result from the incorporation of longer linkages into the pores of polyCOFs. Both the top and cross-section views of SEM images demonstrated the compact and cohesive packing nature of the polyCOF membrane (Figure S32). Exploring other potential linear polymers and COF platforms to construct more polyCOF materials is ongoing in our lab.

Evaluation of the Mechanical Properties of PolyCOF Membranes. Just as in inheriting the crystallinity and porosity of COFs, it is anticipated that the polyCOFs materials would

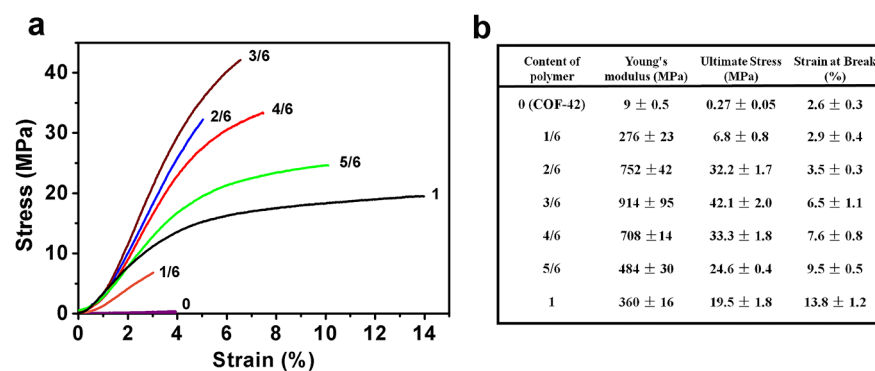


Figure 5. (a) Stress–strain curves of poly_xCOF-42 membranes with different polymer contents ($x = 1/6, 2/6, 3/6, 4/6, 5/6, 1$) compared with the COF-42 membrane. (b) Mechanic analysis of the stress–strain curves in part a.

possess the advantage of linear polymers, e.g., good processability and good mechanical properties. We found that poly_xCOF-42 membranes exhibited high flexibility and excellent processability. The poly_xCOF-42 membranes are able to be cut into any shapes without cracks (Figure S3). The mechanical properties of as-synthesized poly_xCOF-42 membranes were evaluated by tensile tests. As exhibited in the stress–strain curves (Figure 5a), the pristine COF-42 membrane obtained via the traditional interfacial polymerization method was very fragile and possessed a very small ultimate stress (0.26 MPa) and Young's modulus (9 MPa). Interestingly, adopting the polyCOF approach to introduce linear polymers into COF-42 can significantly enhance the mechanical properties of COF membranes when gradually increasing the polymer content (x) from 0 to 3/6. Among these membranes, poly_{3/6}COF-42 membranes achieved the highest ultimate stress of 42.1 MPa and Young's modulus of 914 MPa, which was more than 2 orders of magnitude better than the parent COF-42 membrane. The ultimate stress of polyCOF membranes is higher than all reported COF membranes^{13,37} (Table S4) and comparable to some commercial or classic polymeric membranes (e.g., PVDF,³¹ PIM-1²⁸) (Figure S33). Notably, when increasing the polymer contents (x) from 3/6 to 1, a classic yield behavior was observed in poly_xCOF-42 membranes (Figure 5a). Moreover, the elongation at break for poly_xCOF-42 gradually increased along with the increase of polymer contents. For instance, poly_{5/6}COF-42 can reach ~9.5% strain at break, which is almost 3 times better than parent COF-42 (~2.6%). These results indicate that polymer building blocks play a critical role in improving the mechanical properties of polyCOF membranes.

Actuating Performance of poly_xCOF-42 Membranes.

Responsive materials can rapidly and reversibly change their shapes in response to specific stimuli such as light, electricity, heat, chemical vapors, and pH, which have great potential for applications in sensors, artificial muscle, soft robotics, and intelligent switches.^{38,39} Among them, vapor-responsive actuators that can rapidly and robustly perform large-scale deformation have attracted more and more attention.⁴⁰ To further explore the benefit to incorporate PEGylated polymer into COFs, we found that PEG-based building blocks not only can provide new ways to fabricate a freestanding and flexible COF membrane but also can endow the polyCOF membrane interesting stimuli response properties. It is noteworthy that all poly_xCOF-42 membranes were responsive to common organic solvents with interesting bending behavior (Figure S34). The

poly_{2/6}COF-42 membrane was chosen as a representative to study its vapor-responsive properties in detail. As shown in Figure 6a, when the poly_{2/6}COF-42 membrane was cut into a

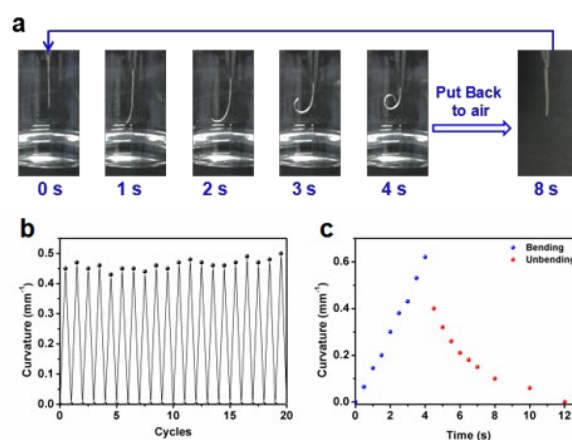


Figure 6. (a) Adaptive movement of the poly_{2/6}COF-42 membrane (2 mm × 13 mm × 11 μm) placed in an ethanol vapor atmosphere (5.8 kPa, 20 °C) and then put back in air (right). (b) Plot showing the reversible deformation of the membrane upon cyclic exposure to ethanol vapor. (c) Plot of curvature against time for the membrane actuator in part a.

rectangle shape and exposed to ethanol vapor ($p = 5.8$ kPa, 20 °C), it bent quickly and formed a closed loop in only ~4 s. When exposed to air, the poly_{2/6}COF-42 membrane can bend back to the initial position within ~8 s. This reversible bending process can undergo >20 cycles without any fatigue (Figure 6b and Movie S3). Furthermore, we also tracked the bending process of poly_{2/6}COF-42 (Figure 6c) and found that the bending curvature increased with time and reached a maximum bending curvature up to 0.62 mm⁻¹ in 4 s. The bending curvature decreased gradually when exposed in air, and then, the membrane recovered its original straight shape. In addition, we also investigated the response behaviors of the poly_{2/6}COF-42 membrane to other vapors such as dichloromethane, acetone, tetrahydrofuran, methanol, and *N,N*-dimethylformamide (Figure S35). The results indicated that the higher vapor pressure induced the faster response. Notably, for the first time, we built a series of solvent-responsive smart COF membranes with reversible shape transformation. The superfast response of polyCOF membranes is comparable to those of previously reported polymer actuators.^{41,42}

To demonstrate if polyCOF membranes can be used as artificial muscles to perform complex movements, a $\text{poly}_{2/6}\text{COF-42}$ actuator was used as an “arm” to lift an object. The bottom of the $\text{poly}_{2/6}\text{COF-42}$ membrane started to bend like an arm when exposed to vapor. We observed that the object (4.5 mg) can be reversibly lifted up to a height of 8.0 mm (Figure 7a). In addition, we also assembled a doll with the



Figure 7. (a) Optical images of the $\text{poly}_{2/6}\text{COF-42}$ membrane used as an artificial arm with a hanging red object. (b) Demonstration that the doll made from the $\text{poly}_{2/6}\text{COF-42}$ membrane can perform a series of complicated movements (e.g., sit-ups) upon exposure to ethanol vapor or air.

$\text{poly}_{2/6}\text{COF-42}$ actuator as its waist and nonresponsive aluminum foil as its other parts. (Figure 7b and Movie S4). Upon exposure to ethanol vapors, the $\text{poly}_{2/6}\text{COF-42}$ part responded to ethanol vapors quickly and induced the doll to perform a “sit-ups” motion. After removal of the ethanol stimulus, the doll gradually recovered to its original shape ascribed to the reversibility of the $\text{poly}_{2/6}\text{COF-42}$ membrane. These movements can be repeated for many cycles without any fatigue.

To better understand the interesting solvent-responsive behavior, the pure PEG20000 polymer ($M_w = 20\,000$ g/mol) and COF-42 membrane were selected as a comparison, respectively. We found that the pure COF-42 membrane did not respond to any vapor, but the PEG20000 membrane (Figure S36) exhibited a bending behavior. These results suggested that the solvent-responsive properties of the $\text{poly}_x\text{COF-42}$ membrane could result from the inhomogeneous expansion of PEGylated polymers upon exposure to vapors.⁴³ However, the responsive rate, sensitivity, and bending curvature of the nonporous PEG20000 membrane were much lower than those of the porous $\text{poly}_x\text{COF-42}$ membrane (Figure S37). The excellent performance of the $\text{poly}_x\text{COF-42}$ membrane can be related to the porous structures of $\text{poly}_x\text{COF-42}$ which can help to adsorb solvent vapors and accelerate the internal mass transport of solvent molecules.⁴⁴ In addition, we found that the vapor-induced expansion always started from the bottom layers of all tested polyCOF membranes which are close to the water solution during interfacial synthesis. It is possibly because the upper layer of polyCOF membranes close to mesitylene solution easily formed a more compact and denser structure with smoother surfaces (Figure 4d). When exposed to vapors, the solvent molecules can diffuse into the less compact bottom layer faster than the upper layer thus inducing the inhomogeneous swelling.⁴¹

CONCLUSION

In conclusion, for the first time, we introduced PEGylated linear polymers as structural building blocks to form a series of defect-free and freestanding polyCOF membranes via a polymer-involved interfacial synthesis method under ambient conditions. Notably, polyCOFs inherited the merits from both COFs (e.g., high crystallinity, permanent porosity, and high stability) and linear polymers (e.g., high flexibility, mechanical strength, and good processability). The crystallinity, porosity, mechanical properties, and thickness of polyCOF membranes can be readily adjusted by changing the synthesis conditions. Moreover, benefiting from the PEGylated linear polymers, polyCOF membranes exhibited excellent mechanical properties and demonstrated an interesting vapor-triggered reversible mechanical response. We first showed that polyCOF membranes can function as artificial muscles to perform various complicated motions, such as lifting objects and doing “sit-ups”. We believe that this new strategy reported herein for fabricating polyCOF membranes can serve as a versatile approach for other linear polymer and COF systems, which will broaden the highly valued applications of COFs and open up new avenues to overcome present limitations.

EXPERIMENTAL SECTION

Syntheses of $\text{poly}_x\text{COF-42}$ Membranes. $\text{poly}_x\text{COF-42}$ membranes were prepared in a 25 mL glass beaker. First, DTH and DTH-400 (total amount: 0.0375 mmol) with different molar ratios were dissolved in the mixture solvent of 1.0 mL of H_2O and 1.0 mL of dioxane as a bottom layer in the beaker. TB (0.025 mmol, 4.0 mg) and 525 μL of CH_3COOH were dissolved in 3.0 mL of mesitylene. This mixture was added into the beaker on top of the hydrazine layer. The reaction was kept at room temperature without disturbance for 48 h. Membranes were formed on the interface and then transferred into CH_3OH . The membranes were washed with CH_3OH in a Soxhlet extractor for 24 h and then dried by a supercritical carbon dioxide dryer.

Safety Statement. No unexpected or unusually high safety hazards were encountered.

ASSOCIATED CONTENT

Supporting Information

The Supporting Information is available free of charge on the ACS Publications website at DOI: 10.1021/acscentsci.9b00212.

Complete experimental procedures, NMR experiment data for new compounds, and additional data and figures including structures, photographs, GPC traces, N_2 adsorption isotherms, PXRD patterns, FT-IR spectra, ^{13}C NMR spectra, SEM images, TEM images, pore size distributions, absorbance results, and BET plots (PDF) Movie S1: pristine COF-42 (without adding DTH-400) formed an opaque and brittle membrane which was apt to break or crack during bending process (AVI) Movie S2: $\text{poly}_{2/6}\text{COF-42}$ membrane repeatedly bent, twisted, or stretched without damage (AVI) Movie S3: $\text{poly}_{2/6}\text{COF-42}$ membrane can bend back to the initial position within ~ 8 s, and the process can undergo >20 cycles without any fatigue (AVI) Movie S4: assembled doll with the $\text{poly}_{2/6}\text{COF-42}$ actuator as its waist and nonresponsive aluminum foil as its other parts (AVI)

■ AUTHOR INFORMATION

Corresponding Authors

*E-mail: chenyaoyao@nankai.edu.cn.

*E-mail: zhangzhenjie@nankai.edu.cn.

*E-mail: sqma@usf.edu.

ORCID 

Jiajie Liang: 0000-0003-2112-6721

Fusheng Pan: 0000-0002-4941-1295

Peng Cheng: 0000-0003-0396-1846

Yao Chen: 0000-0002-3465-7380

Shengqian Ma: 0000-0002-1897-7069

Zhenjie Zhang: 0000-0003-2053-3771

Author Contributions

The manuscript was written through contributions of all authors. All authors have given approval to the final version of the manuscript.

Notes

The authors declare no competing financial interest.

■ ACKNOWLEDGMENTS

The authors acknowledge the financial support from the National Natural Science Foundation of China (21601093), Tianjin Natural Science Foundation of China (17JCZDJC37200), and NSF (CBET-1706025).

■ REFERENCES

- (1) Bisbey, R. P.; Dichtel, W. R. Covalent Organic Frameworks as a Platform for Multidimensional Polymerization. *ACS Cent. Sci.* **2017**, *3* (6), 533–543.
- (2) Ding, S. Y.; Wang, W. Covalent organic frameworks (COFs): from design to applications. *Chem. Soc. Rev.* **2013**, *42* (2), 548–568.
- (3) Feng, X.; Ding, X.; Jiang, D. Covalent organic frameworks. *Chem. Soc. Rev.* **2012**, *41* (18), 6010–6022.
- (4) Diercks, C. S.; Yaghi, O. M. The atom, the molecule, and the covalent organic framework. *Science* **2017**, *355* (6328), eaal1585.
- (5) Baldwin, L. A.; Crowe, J. W.; Pyles, D. A.; McGrier, P. L. Metalation of a Mesoporous Three-Dimensional Covalent Organic Framework. *J. Am. Chem. Soc.* **2016**, *138* (46), 15134–15137.
- (6) Song, Y.; Sun, Q.; Aguila, B.; Ma, S. Opportunities of Covalent Organic Frameworks for Advanced Applications. *Adv. Sci.* **2019**, *6*, 1801410.
- (7) Zeng, Y.; Zou, R.; Luo, Z.; Zhang, H.; Yao, X.; Ma, X.; Zou, R.; Zhao, Y. Covalent organic frameworks formed with two types of covalent bonds based on orthogonal reactions. *J. Am. Chem. Soc.* **2015**, *137* (3), 1020–1023.
- (8) Wang, X.; Han, X.; Zhang, J.; Wu, X.; Liu, Y.; Cui, Y. Homochiral 2D Porous Covalent Organic Frameworks for Heterogeneous Asymmetric Catalysis. *J. Am. Chem. Soc.* **2016**, *138* (38), 12332–12335.
- (9) Sun, Q.; Aguila, B.; Perman, J.; Nguyen, N.; Ma, S. Flexibility Matters: Cooperative Active Sites in Covalent Organic Framework and Threaded Ionic Polymer. *J. Am. Chem. Soc.* **2016**, *138* (48), 15790–15796.
- (10) Fu, J.; Das, S.; Xing, G.; Ben, T.; Valtchev, V.; Qiu, S. Fabrication of COF-MOF Composite Membranes and Their Highly Selective Separation of H₂/CO₂. *J. Am. Chem. Soc.* **2016**, *138* (24), 7673–7680.
- (11) Zeng, Y.; Zou, R.; Zhao, Y. Covalent Organic Frameworks for CO₂. *Adv. Mater.* **2016**, *28* (15), 2855–2873.
- (12) Mitra, S.; Sasmal, H. S.; Kundu, T.; Kandambeth, S.; Illath, K.; Diaz Diaz, D.; Banerjee, R. Targeted Drug Delivery in Covalent Organic Nanosheets (CONs) via Sequential Postsynthetic Modification. *J. Am. Chem. Soc.* **2017**, *139* (12), 4513–4520.
- (13) Khayum M, A.; Vijayakumar, V.; Karak, S.; Kandambeth, S.; Bhadra, M.; Suresh, K.; Acharambath, N.; Kurungot, S.; Banerjee, R.

Convergent Covalent Organic Framework Thin Sheets as Flexible Supercapacitor Electrodes. *ACS Appl. Mater. Interfaces* **2018**, *10* (33), 28139–28146.

(14) Sun, Q.; Aguila, B.; Perman, J.; Butts, T.; Xiao, F.-S.; Ma, S. Integrating Superwettability within Covalent Organic Frameworks for Functional Coating. *Chem.* **2018**, *4*, 1726–1739.

(15) Cote, A. P.; Benin, A. I.; Ockwig, N. W.; O’Keeffe, M.; Matzger, A. J.; Yaghi, O. M. Porous, crystalline, covalent organic frameworks. *Science* **2005**, *310* (5751), 1166–1170.

(16) Segura, J. L.; Mancheno, M. J.; Zamora, F. Covalent organic frameworks based on Schiff-base chemistry: synthesis, properties and potential applications. *Chem. Soc. Rev.* **2016**, *45* (20), 5635–5671.

(17) Uribe-Romo, F. J.; Doonan, C. J.; Furukawa, H.; Oisaki, K.; Yaghi, O. M. Crystalline covalent organic frameworks with hydrazone linkages. *J. Am. Chem. Soc.* **2011**, *133* (30), 11478–11481.

(18) Jin, E.; Asada, M.; Xu, Q.; Dalapati, S.; Addicoat, M. A.; Brady, M. A.; Xu, H.; Nakamura, T.; Heine, T.; Chen, Q.; Jiang, D. Two-dimensional sp² carbon-conjugated covalent organic frameworks. *Science* **2017**, *357* (6352), 673–676.

(19) Zhuang, X.; Zhao, W.; Zhang, F.; Cao, Y.; Liu, F.; Bi, S.; Feng, X. A two-dimensional conjugated polymer framework with fully sp²-bonded carbon skeleton. *Polym. Chem.* **2016**, *7*, 4176–4181.

(20) Vazquez-Molina, D. A.; Mohammad-Pour, G. S.; Lee, C.; Logan, M. W.; Duan, X.; Harper, J. K.; Uribe-Romo, F. J. Mechanically Shaped Two-Dimensional Covalent Organic Frameworks Reveal Crystallographic Alignment and Fast Li-Ion Conductivity. *J. Am. Chem. Soc.* **2016**, *138* (31), 9767–9770.

(21) Fan, H.; Gu, J.; Meng, H.; Knebel, A.; Caro, J. High-Flux Membranes Based on the Covalent Organic Framework COF-LZU1 for Selective Dye Separation by Nanofiltration. *Angew. Chem., Int. Ed.* **2018**, *57* (15), 4083–4087.

(22) Dey, K.; Pal, M.; Rout, K. C.; Kunjattu, H. S.; Das, A.; Mukherjee, R.; Kharul, U. K.; Banerjee, R. Selective Molecular Separation by Interfacially Crystallized Covalent Organic Framework Thin Films. *J. Am. Chem. Soc.* **2017**, *139* (37), 13083–13091.

(23) Matsumoto, M.; Valentino, L.; Stiehl, G. M.; Balch, H. B.; Corcos, A. R.; Wang, F.; Ralph, D. C.; Mariñas, B. J.; Dichtel, W. R.; Wang, F.; Ralph, D. C.; Mariñas, B. J.; Dichtel, W. R. Lewis-Acid-Catalyzed Interfacial Polymerization of Covalent Organic Framework Films. *Chem.* **2018**, *4* (2), 308–317.

(24) Shao, P.; Li, J.; Chen, F.; Ma, L.; Li, Q.; Zhang, M.; Zhou, J.; Yin, A.; Feng, X.; Wang, B. Flexible Films of Covalent Organic Frameworks with Ultralow Dielectric Constants under High Humidity. *Angew. Chem., Int. Ed.* **2018**, *57* (50), 16501–16505.

(25) Zhang, W.; Zhang, L.; Zhao, H.; Li, B.; Ma, H. A two-dimensional cationic covalent organic framework membrane for selective molecular sieving. *J. Mater. Chem. A* **2018**, *6* (27), 13331–13339.

(26) Kandambeth, S.; Biswal, B. P.; Chaudhari, H. D.; Rout, K. C.; Kunjattu, H. S.; Mitra, S.; Karak, S.; Das, A.; Mukherjee, R.; Kharul, U. K.; Banerjee, R. Selective Molecular Sieving in Self-Standing Porous Covalent-Organic-Framework Membranes. *Adv. Mater.* **2017**, *29* (2), 1603945.

(27) Halder, A.; Ghosh, M.; Khayum, M. A.; Bera, S.; Addicoat, M.; Sasmal, H. S.; Karak, S.; Kurungot, S.; Banerjee, R. Interlayer Hydrogen-Bonded Covalent Organic Frameworks as High-Performance Supercapacitors. *J. Am. Chem. Soc.* **2018**, *140* (35), 10941–10945.

(28) McKeown, N. B.; Budd, P. M. Polymers of intrinsic microporosity (PIMs): organic materials for membrane separations, heterogeneous catalysis and hydrogen storage. *Chem. Soc. Rev.* **2006**, *35* (8), 675–683.

(29) Basu, S.; Khan, A. L.; Cano-Odena, A.; Liu, C.; Vankelecom, I. F. Membrane-based technologies for biogas separations. *Chem. Soc. Rev.* **2010**, *39* (2), 750–768.

(30) Marchetti, P.; Jimenez Solomon, M. F.; Szekeley, G.; Livingston, A. G. Molecular separation with organic solvent nanofiltration: a critical review. *Chem. Rev.* **2014**, *114* (21), 10735–10806.

(31) Denny, M. S., Jr.; Cohen, S. M. In Situ Modification of Metal-Organic Frameworks in Mixed-Matrix Membranes. *Angew. Chem., Int. Ed.* **2015**, *54* (31), 9029–9032.

(32) Dechnik, J.; Gascon, J.; Doonan, C. J.; Janiak, C.; Sumbly, C. J. Mixed-Matrix Membranes. *Angew. Chem., Int. Ed.* **2017**, *56* (32), 9292–9310.

(33) Vu, D. Q.; Koros, W. J.; Miller, S. J. Mixed matrix membranes using carbon molecular sieves I. Preparation and experimental results. *J. Membr. Sci.* **2003**, *211* (2), 311–334.

(34) Zhang, Z.; Nguyen, H. T.; Miller, S. A.; Cohen, S. M. polyMOFs: A Class of Interconvertible Polymer-Metal-Organic-Framework Hybrid Materials. *Angew. Chem., Int. Ed.* **2015**, *54* (21), 6152–6157.

(35) Ding, S. Y.; Cui, X. H.; Feng, J.; Lu, G.; Wang, W. Facile synthesis of -C = N- linked covalent organic frameworks under ambient conditions. *Chem. Commun.* **2017**, *53* (87), 11956–11959.

(36) Zhang, G.; Hong, Y.-l.; Nishiyama, Y.; Bai, S.; Kitagawa, S.; Horike, S. Accumulation of Glassy Poly(ethylene oxide) Anchored in a Covalent Organic Framework as a Solid-State Li⁺ Electrolyte. *J. Am. Chem. Soc.* **2019**, *141* (3), 1227–1234.

(37) Sasmal, H. S.; Aiyappa, H. B.; Bhange, S. N.; Karak, S.; Halder, A.; Kurungot, S.; Banerjee, R. Superprotonic Conductivity in Flexible Porous Covalent Organic Framework Membranes. *Angew. Chem., Int. Ed.* **2018**, *57* (34), 10894–10898.

(38) Jamal, M.; Zarafshar, A. M.; Gracias, D. H. Differentially photo-crosslinked polymers enable self-assembling microfluidics. *Nat. Commun.* **2011**, *2*, 527.

(39) Stuart, M. A.; Huck, W. T.; Genzer, J.; Muller, M.; Ober, C.; Stamm, M.; Sukhorukov, G. B.; Szleifer, I.; Tsukruk, V. V.; Urban, M.; Winnik, F.; Zauscher, S.; Luzinov, I.; Minko, S. Emerging applications of stimuli-responsive polymer materials. *Nat. Mater.* **2010**, *9* (2), 101–113.

(40) Deng, H.; Dong, Y.; Zhang, C.; Xie, Y.; Zhang, C.; Lin, J. An instant responsive polymer driven by anisotropy of crystal phases. *Mater. Horiz.* **2018**, *5*, 99–107.

(41) Zhang, L.; Naumov, P.; Du, X.; Hu, Z.; Wang, J. Vapomechanically Responsive Motion of Microchannel-Programmed Actuators. *Adv. Mater.* **2017**, *29* (37), 1702231.

(42) Huang, H. W.; Sakar, M. S.; Petruska, A. J.; Pane, S.; Nelson, B. J. Soft micromachines with programmable motility and morphology. *Nat. Commun.* **2016**, *7*, 12263.

(43) Salvekar, A. V.; Huang, W. M.; Xiao, R.; Wong, Y. S.; Venkatraman, S. S.; Tay, K. H.; Shen, Z. X. Water-Responsive Shape Recovery Induced Buckling in Biodegradable Photo-Cross-Linked Poly(ethylene glycol) (PEG) Hydrogel. *Acc. Chem. Res.* **2017**, *50* (2), 141–150.

(44) Zhao, Q.; Dunlop, J. W.; Qiu, X.; Huang, F.; Zhang, Z.; Heyda, J.; Dzubiella, J.; Antonietti, M.; Yuan, J. An instant multi-responsive porous polymer actuator driven by solvent molecule sorption. *Nat. Commun.* **2014**, *5*, 4293.